International Journal of Research
Available at https://edupediapublications.org/journals
p-ISSN: 2348-6848
e-ISSN: 2348-795X
Volume 02 Issue 01
January 2015

Analysis Of Rectangular Resonant Microstrip Antenna Loaded With Metamaterial And A Slot Loaded Rectangular Microstrip Antenna

SHIVARAM PORIKA[1] ,A ARUNKUMAR[2]

[1&2]assistant professor

Vaageswari College of engineering, karimnagar, Telangana.

[1]shivaram420@gmail.com,[2]arunraj.akula@gmail.com

ABSTRACT: Authors analyze a slot loaded rectangular micro-strip patch antenna and a sub-wavelength compact, resonant patch antenna loaded with metamaterial. The slot is taken as capacitive reactance on the patch. It is found that the resonance frequency decreases with increasing slot width for a given slot length the decrease in the resonance frequency in the lighter side for longer slot length, where as it is in the min. side for the lower slot length, in case of resonant patch antenna loaded with metamaterial the matching and radiation properties have analyzed. It is shown how these configurations may exhibit in principle an arbitrarily low resonant frequency for a fixed dimension, but they may necessarily radiate efficiently when their size is electrically small.

Keywords: Microstrip antennas, Meta material

I. INTRODUCTION

Demand for compact radiators with sufficiently high gain is rapidly increasing in many application areas, as modern wireless telecommunication systems and space communications require compact antennas with high gain, which become even more relevant requirements when the radiating elements have to be combined in large antenna arrays for satellites, space vehicles, airplanes, and so on. Microstrip antennas, due to their inherent capabilities (mainly low cost, low weight and low profile) are widely used in those setups [1], [2]. Even though such antennas are very thin compared to the operating wavelength (0.05-0.01 λ) in their cross section, however, still their transverse dimensions cannot be made arbitrarily short, since a regular patch antenna resonates at a given frequency when its linear transverse dimension is of the order of half wavelength. The interest in overcoming this limitation represents one of the main challenges for antenna designers. In this context of novel artificial materials

an important role may be played by metamaterials, which, due to their interesting anomalous electromagnetic features, have attracted a great deal of attention in recent years for several electromagnetic applications [3]. Interest is focused in the presented paper on a typical wave interaction of metamaterials with anomalous electromagnetic constitutive parameters, and in particular with negative real part of their permittivity [Є - negative ENG)], of their permeability [μ -negative (MNG)] or with both these quantities being negative [double-negative (DNG)] in a specific frequency range. The phase compensation properties of DNG metamaterials may allow synthesizing sub wavelength cavity resonators [4], waveguides [5] and scatterers [6] with resonant properties essentially independent on their effective physical size. In the quasi-static limit, when the retardation effects are negligible due to the small dimensions of such components and only one of the two constitutive parameters interact with the field depending on its polarization, even single negative (SNG) materials, i.e., ENG or MNG, may be utilized to achieve similar effects. Such sub-wavelength resonances may be applied also to antenna configurations. In the present paper, we have comparatively analyzed the rectangular antenna loaded with metamaterial and fed with microstrip line by thoroughly revisit the theory of patch antennas in terms of resonance frequency and VSWR with respect to slot length and slot width with the help of equivalent circuit diagram to show how suitable pairing of metamaterials and standard dielectrics may indeed allow a sub-wavelength resonance in such structures. Necessary and sufficient conditions are determined to get such quasi-static resonances for patch antenna setups. Then, the radiation properties of such sub-wavelength patches are studied theoretically, showing which configurations may be designed to properly radiate in free space. Finally, some optimized designs are verified through full-wave numerical simulations, taking into account dispersion, losses and feeding networks for these devices.

2.THEORETICALCONSIDERATONS

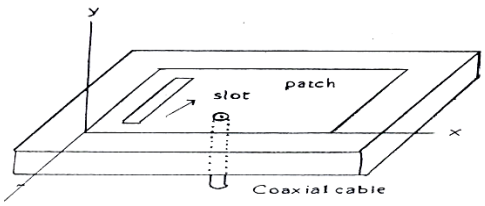

Fig.1. Geometry of slot loaded rectangular microstrip antenna

Equivalent circuits

The equivalent circuit of slot-loaded rectangular microstrip antenna is

presented in Fig 2.where R_1, L_1, C_1 of patch are given by

$$C_1=\frac{\varepsilon_e\varepsilon_0 LW}{2h}\cos^{-2}\left(\frac{\pi z_0}{L}\right);\qquad L_1=\frac{1}{C_1\omega_r^2};\qquad \& R_1=\frac{Q}{\omega_r C_1} \tag{1}$$

It may be noted that input impedance (Z_{in}) of the circuit in Fig2 a. Excluding slot can be expressed as

$$Z_{in}=\frac{1}{\frac{1}{R_1}+j\omega C_1+\frac{1}{j\omega L_1}}=\frac{R1(\omega L_1)^2}{(\omega L_1)^2+R_1^2\left(\omega^2 L_1C_1-1\right)^2}-j\frac{R_1^2\,\omega L_1\left(\omega^2 L_1C_1-1\right)}{(\omega L_1)^2+R_1^2\left(\omega^2 L_1C_1-1\right)^2} \tag{2}$$

The input impedance of the slot-loaded patch can be calculated from Fig. 2b as

$$Z_{ins}=\frac{(R-jX)(jX_s)}{R-jX+jX_s}$$

$$Z_{ins}=\frac{X.X_s+jR.X_s}{R-j(X-X_s)} \tag{3}$$

Using this value, the reflection coefficient, VSWR and return loss can be computed

Reflection coefficient

$$(\Gamma)=\frac{Z_0-Z_{ins}}{Z_0+Z_{ins}} \tag{4}$$

Where $Z_0=$ characteristic impedance of the co-axial feed (50 ohm)

$$VSWR=S=\frac{1+|\Gamma|}{1-|\Gamma|} \tag{5}$$

and Return loss $=20\log|\Gamma|$ (6)

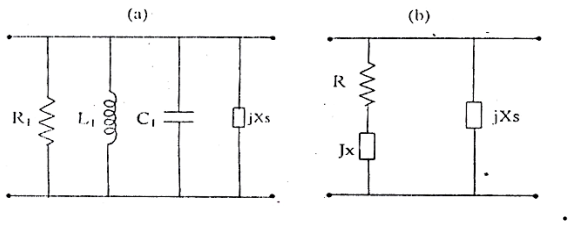

Fig.2 Equivalent circuits.

III. CALCULATIONS

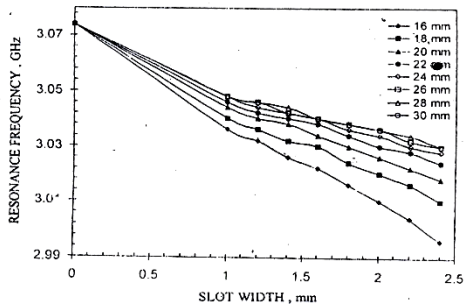

Fig.3. Variation of resonance frequency with slot width

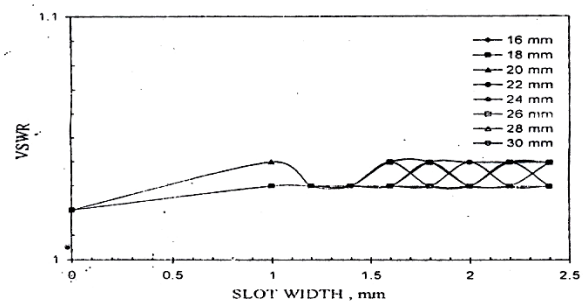

Fig.4. Variation of VSWR with slot width for different slot lengths

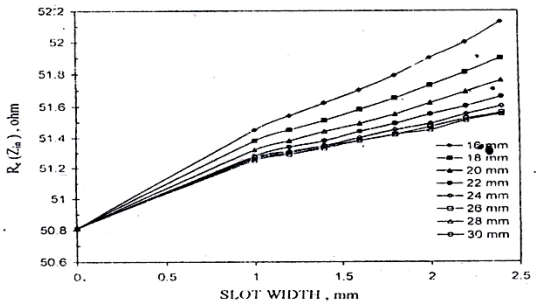

Fig.5. Variation of Re (Z_{in}) with slot width for different slot lengths

As resonance frequency increases the slot width of patch also increases (fig.3).An uniform variation in voltage standing wave ratio has been analyzed on the slot-width greater than 1.5mm (fig4).

IV. RESONANT FREQUENCIES AND RADIATION PROPERTIES

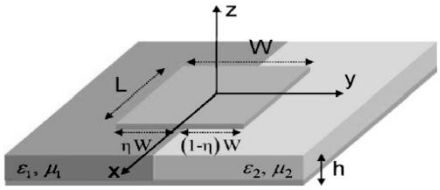

Fig.6 A rectangular patch antenna loaded with transversally inhomogeneous substrate.

Consider the rectangular patch antenna depicted in Fig. 6. It consists of a metallic patch with transverse dimensions $L \times W$ placed over a ground plane (distant h). The underneath substrate is inhomogeneous, filled with two isotropic and homogeneous materials with permittivity and permeability, $\varepsilon_1(w)\mu_1(w)$ and $\varepsilon_2(w)\mu_2(w)$, in general varying with frequency (an e^{jwt} notation is adopted in the following). The quantity η represents the filling ratio of the volume underneath the patch, as described in the figure. The antenna is embedded in a suitable Cartesian reference system, as defined in the figure, and it radiates in free space, with permittivity and permeability $\varepsilon_\circ \mu_\circ$ .The resonant frequencies of the radiator in Fig. 6 may be evaluated with good

approximation by applying a standard cavity model [7], [8]. The resonant frequencies of the equivalent cavity for the modes may be easily obtained by applying all the boundary conditions, and they correspond to the solution of the following dispersion equation:

$$\frac{k_1}{\omega\mu_1}\tan[k_1\eta W] = -\frac{\omega\varepsilon_2}{k_2}\tan[k_2(1-\eta)W] \quad (7)$$

Where $k_i = \omega\sqrt{\varepsilon_i\mu_i}$ with i = 0,1,2.

Substituting the tangent functions with their arguments under the assumption of sub- wavelength size of the patch, i.e. ,W,<<min[$2\pi/k_1$, $2\pi/k_2$] ,yields the approximate equation:

$$\eta/1-\eta \approx -\varepsilon_2/\varepsilon_1 \quad (8)$$

If one hypothetically assumes that $\varepsilon_1$and ε_2 are independent of frequency (which they are not, [9]), this expression is surprisingly independent of *w* and *W*, implying that in the first approximation the patch of Fig.6 may resonate at any arbitrarily low frequency for any arbitrarily small width of the patch, provided that the previous equality among the filling ratio η and the permittivity's of the two materials is satisfied. In other words, two permittivity's are oppositely signed in the two materials, since0< η<1, makes the left-hand side of (8) a strictly positive quantity. Clearly, in fact, such a patch cannot resonate at low frequency unless special metamaterials are employed.

The fact that an ENG, MNG or DNG material is necessarily dispersive with frequency [8] ensures the indirect dependence of the previous dispersion relation on frequency. These findings, consistent with the sub-wavelength cavities, waveguides, scatterers and antennas described in [4], for which again a filling ratio factor, rather than their total size, determines the resonance of the system, may be justified by noticing that at the interface between materials with oppositely signed permittivity's and/or permeability's a local plasmonic resonance arises, which, if properly designed, may induce a resonance in the whole component. due to the polarization of the mode under analysis (TM_{0m0},with electric field E_Z and H_Z magnetic field tangential to the interface) and due to the magnetic boundary conditions at the side walls of the cavity, in the quasi-static limit in which (8) applies the permittivity's play a dominant role in the possibility of achieving such quasi-static resonance. Applying the dispersion relation given by (7), it is possible to determine the resonant frequencies of a given patch varying its medium loading. Fig. 7, as an example, shows the resonant frequency variation, as solution of (7), for a patch of width W==50 mm with η =0.5 having one of the two media being a DPS material with $\varepsilon_1=\varepsilon_0$, $\mu_1=\mu_0$ and varying permittivity of the other material ε_2.

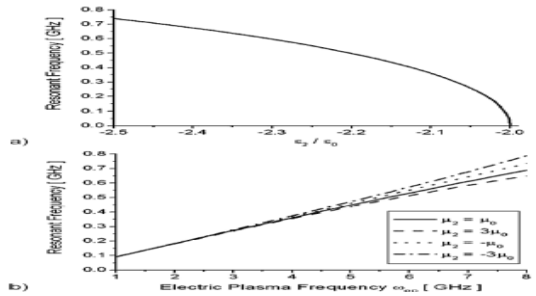

Fig. 7. (a) Variation of the resonant frequency of the rectangular patch antenna of Fig.6 with W = 50mm, η = 0:5, $\varepsilon_1 = 2\ \varepsilon_0$, $\mu_{1=}\ \mu_2 = \mu_0$ as a function of ε_2 . (b)

the same as a function of the electric plasma frequency of a Drude-like dispersive metamaterial for the second medium, varying also its permeability μ_2 as a parameter. In particular, Fig. 7(a) shows the variation of the resonant frequency with assuming $\mu_{2=}\mu_0$, whereas Fig. 7(b) shows resonance frequency variation versus the plasma frequency the resonance frequency variation versus the plasma frequency w_{ep} assuming a Drude dispersive material for the permittivity of the loading ENG material, *i.e.* In this second case μ_2, is also varied as a parameter.

When the filling material is homogeneous, *i.e.* $\varepsilon_1 = \varepsilon_2 = 2\ \varepsilon_0$, the patch has its resonance at $f=w/2\pi$ =2.12GHz. However, loading the patch with an ENG material can reduce the resonance frequency in principle without limits, as shown in Fig. 7(a). Fig. 7(b) relates this variation to the plasma frequency of a Drude-like dispersive material. This has been adopted to model the realistic dispersion of an ENG metamaterial made by embedding specific inclusions inside a host material. Also in this case, properly varying the size and shape of the inclusions that form the second filling material. in order to approach the effective permittivity of $\varepsilon_2 = -2\ \varepsilon_0$, the resonance frequency may in principle be brought down arbitrarily. These results, as Fig. 7(b) shows, are weakly affected by the permeability of the second material μ_2, and this dependence becomes irrelevant when the resonant frequency is reduced, since the quasi-static approximation represented by (19) holds. A filling material with high electric permittivity may be employed instead of such plasmonic metamaterial.

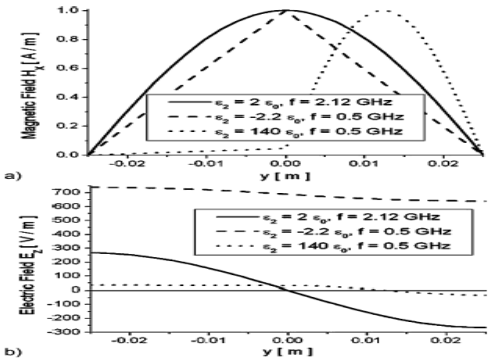

Fig.8. Variation of the (a) magnetic and (b) electric fields underneath the rectangular patch antenna of Fig.7, at resonance, with: $\varepsilon_2 = 2\ \varepsilon_0$, (solid line), resonating at f = 2:12 GHz; ε_2 = -2.2 ε_0,(dashed line), resonating at f = 0:5GHz; $\varepsilon_2 = 140\ \varepsilon_0$, (dotted line), resonating at f = 0:5 GHz. This solution,

however, is intrinsically limited by the fact that a higher permittivity usually accompanies higher losses and the presence of surface waves, and reducing the resonance frequency to very low values would require the use of extremely high permittivities. On the other hand, the resonance is not obtained by adjusting the wavelength in the filling material, but instead by inducing a plasmonic resonance at the interface underneath the patch, which allows a phase cancellation similar to the effect predicted in [4]. This point is further clarified in Fig. 8, which shows the electric and magnetic field distribution at resonance predicted by the cavity model for the patch considered in Fig. 7 for the three cases when: (solid line) $\varepsilon_2 = 2\ \varepsilon_0$, , i.e., when the substrate is homogeneous and the patch resonates at f = 2.12GHz; (dashed line) for a second material chosen according to (7) to lower the patch resonance to f = 0.5 GHz, i.e., using a material with ε_2 $(f = 0.5\text{GHz}) = -2.2\ \varepsilon_0$; (dotted line) for a second material with its permittivity increased so that the patch can resonate at the frequency f = 0.5GHz, i.e., with $\varepsilon_2 = 140\ \varepsilon_0$.

The magnetic field amplitudes have been normalized in the fig 8 to their relative maximum and the electric field are normalized accordingly for comparison. As it can be seen, the three cases show very different properties. The standard resonance of the patch would happen at f = 2.12GHz, as the solid line shows.

At this frequency the patch width is 0.5 λ, with λ being the wavelength inside the homogeneous material loading the patch. As it is well known, the magnetic field in fact experiences a half-wavelength sinusoidal variation from one side to the other of the patch, whereas the electric field flips its sign, with a 180^0 phase variation. Filling the region $y>0$ with a material with ε_2 $(f = 0.5\text{GHz}) = -2.2\ \varepsilon_0$ allows getting a resonance at $f = 0.5\text{GHz}$, as shown by the dashed line.

In this case the magnetic field flips the sign of its derivative, due to the boundary conditions at the interface between the two "oppositely signed" materials, and this allows to shrink the electrical dimensions of the equivalent cavity. As clearly seen in the figure, the electric field variation in this case is almost constant and its phase does not flip passing from one side to the other of the patch.

This affects the radiation properties of the patch. Employing a high-dielectric material (dotted line), the resonance frequency is made low by decreasing the wavelength in the material in $y>0$, which in fact is responsible for almost all the sinusoidal variation of the magnetic field.

The electric field remains almost constant in the left material, but experiences a 180^0 phase shift in the material with high permittivity. The well-known cause of

radiation is represented by the fringing electric field at the two sides of the patch, *i.e.*, at $y = \pm$ ½ w. They correspond to the equivalent magnetic currents $k = \hat{n} \times E \big|_{y=\pm w/2}$, where E is the electric field at $y = \pm$ ½ w , as predicted by

the cavity model, and is the normal to the side of the patch, *i.e.* $\hat{n} = \pm\hat{x}$ respectively. In the solid and dotted line cases, *i.e.*, when the cavity is resonating in a conventional way, the electric field on the two sides of the patch is oppositely oriented, and therefore the two sides of the patch radiate in phase towards broadside this ensures the conventionally shaped radiation pattern of the patch antenna, with reasonable directivity at broadside. In the dot-line case, when a high permittivity is employed to squeeze the patch width, we may expect a lower directivity, due to the reduced electrical distance between the two radiating edges, and a lowered gain caused by the presumably strong excitation of surface waves, due to the presence of a high- substrate. Also the potential presence of high losses in such material would contribute to deterioration of its radiating performance. When the patch is loaded with a metamaterial, however, the mode excited (dashed line) will cause the two sides of the patch to radiate out of phase. Due to the electrically small dimensions of the patch, moreover, the two magnetic currents almost cancel each other for all the visible angles, and thus the radiation efficiency of such an antenna would be very poor. Another aspect should also be considered: the interfaces at *y=0* and

$$\begin{cases} x = 0 \\ y > 0 \end{cases}$$

support surface plasmons, since they are interfaces between media with materials with opposite permittivities [12]. If the plasmonic resonance at is the main factor responsible for the sub-wavelength resonance, these surface plasmons, when excited, would eventually trap some energy from the source, thus further reducing the radiation efficiency of the antenna.

V.NUMERICAL ANALYSIS

As a first example, behavior of the rectangular patch antenna of Fig. 7 is atudied, *with* W = 50 mm.,L=40 mm ,h=1.5 mm, η = 0:5, $\varepsilon_1 = 2\ \varepsilon_0$, $\mu_{1=}\ \mu_{2\,=}\ \mu_0$, properly loaded with a Drude dispersive and lossy ENG material with $\varepsilon_2(\omega) = \varepsilon_0 (1-\omega_{ep}^2 /[\ \omega(\omega-j\ \omega_\tau)\ ]\ )$. The plasma frequency has been set at w_{ep} =5.6GHz to get ε_2*(f* = 0.5GHz*)* $\approx$ 2.2 ε_0, which may be obtained in an artificial metamaterial by embedding properly designed conducting wires oriented along *z* in vacuum or another dielectric [10], [11]. Losses in the metamaterial have also been added to reflect the possible ohmic losses in the conducting inclusions, and thus the damping frequency in the Drude model has been set at w_τ =50 MHz. The antenna is fed by a coaxial probe placed at the position X_p=0, y_p= –w/4, with inner radius of r_{in}=0.3 mm. and characteristic impedance Z_p = 125Ω. Also finite substrate and ground pane have been considered, both with total size of 100×100 mm². In order to consider all the realistic aspects of the design, the finiteness of the metal thickness has also been modeled, fixing it at 0.01 mm. The return loss and the input impedance are plotted in Fig.9, showing two distinct resonances *f* = 0.48GHz at *f* = 2.44GHz, with good agreement with the cavity model.

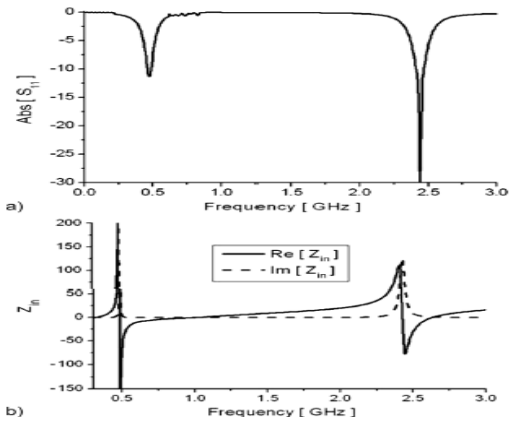

Fig.9 . Full-wave numerical simulation results for (a) return loss and (b) input impedance of the antenna in Fig. 7 with a Drude material with losses, fed by a coaxial cable, as described in the text.

The sub-wavelength resonance in this case is poorly matched.

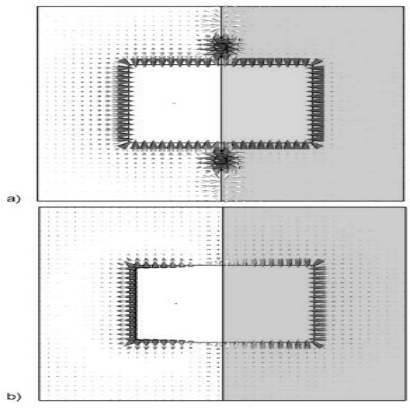

Fig.10 (Results calculated using CST Microwave Studio [13]). Electric field distribution (snapshot in time, top view) at the first two resonant frequencies for the antenna of Fig. 9: at (a) f = 0:48 GHz and (b) f = 2:44 GHz.

Fig. 10 reports the electric field distribution for these two different resonance frequencies on the plane of the patch.

This clearly shows how the fringing fields are oppositely directed in the sub-wavelength case, different from the usual resonance at f = 2.44GHz. The field distributions are consistent with the cavity model analysis described in the previous section and confirm the different behavior of the field at the radiating edges at the two frequencies, highlighting also the standing waves present at the interface y = 0 due to the excitation of surface plasmons. The radiation patterns in the two cases are substantially different, since at the lower frequency the patch is not radiating properly and it shows a nullat broadside and an insufficient gain over all the visible angles.

This rectangular configuration at the frequency f = 0.48GHz ends up being a good candidate for a matching network for the excitation of surface plasmons at the interface y = 0 rather than as a good radiator.

VI. CONCLUSION

It may be concluded that loading of patch with narrow slot. Affects significantly resonance frequency. input impedance and bandwidth increase with slot with for a given slot length. we have analyzed the possibility of designing sub wavelength resonant patch antennas using metamaterial blocks. Realistic numerical

simulations, considering material dispersion, losses and the presence of the feeding network have been also presented, providing a validation of the theoretical results and showing how a practical realization is foreseeable. While as with the equilateral triangular microstrip antenna with microstrip feed it is found that 35.5% of space can be save is constructing ETMP structure. This may indeed open interesting venues for the design of small-scaled antennas with enhanced performance.

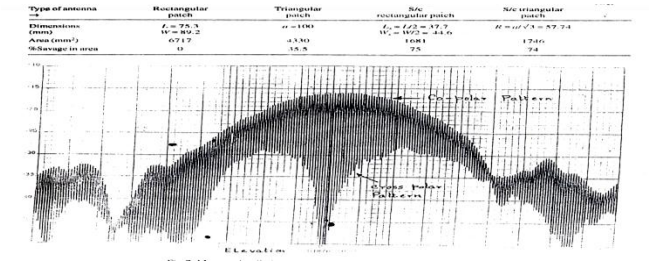

Fig.11.Comparison of occupied aperture area of

rectangular & triangular patch configuration: h=1.6mm & ε_r=2.22 at f_r =1325 MHz**.**

VII. REFERENCES

[1] D. M. Pozar and D. H. Schaubert, *Microstrip Antennas: The Analysis and Design of Microstrip Antennas and Arrays*. New York: IEEE Press, 1995.

[2] J. R. James and P. S. Hall, *Handbook of Microstrip Antennas*.London, U.K.: Peter Peregrinus, 1989.

[3] R. W. Ziolkowski and N. Engheta, Eds., *IEEE Trans. Antennas Propag., Special Issue on Metamaterials*, vol. 51, pp. 2546–2750, Oct. 2003.

[4] N. Engheta, "An idea for thin subwavelength cavity resonators using metamaterials with negative permittivity and permeability," *IEEE Antennas Wireless Propag. Lett.*, vol. 1, no. 1, pp.10–13, 2002.

[5] A. Alù and N. Engheta, "Guided modes in a waveguide filled with a pair of single-negative (SNG), double-negative (DNG), and/or double-positive (DPS) layers," *IEEE Trans. Microw. Theory Tech.*, vol. MTT-52, no. 1, pp. 199–210, Jan. 2004.

[6]"Polarizabilities and effective parameters for collections of spherical nano-particles formed by pairs of concentric double-negative (DNG), single-negative (SNG) and/or double-positive (DPS) metamaterial layers," *J. Appl. Phys.*, vol. 97, May 1, 2005, 094310.

[7] K. R. Carver and J. W. Mink, "Microstrip antenna technology," *IEEE Trans. Antennas Propag.*, vol. AP-29, no. 1, pp. 2–24, Jan. 1981.

[8] W. F. Richards, Y. T. Lo, and D. D. Harrison "An improved theory of microstrip antennas with applications," *IEEE Trans. Antennas Propag.*, vol. AP-29, no. 1, pp. 34–46, Jan. 1981.

[9] L. Landau and E. M. Lifschitz, *Electrodynamics of Continuous Media*. Oxford, U.K.: Pergamon Press, 1984.

[10] W. Rotman, "Plasma simulation by artificial dielectrics and parallelplate media," *IRE Trans. Antennas Propag.*, pp. 82–84, 1962.

[11] J. B. Pendry, A. J. Holden, D. J. Robbins, and W. J. Stewart, "Lowfrequency plasmons in thin wire structures," *J. of Physics: Condensed Matter*, vol. 10, pp. 4785–4809, 1998.

[12] J. D. Jackson, *Classical Electrodynamics*. New York: Wiley, 1975.

[13] CST Microwave Studio 5.0 CST of America [Online].Available: http:// www.cst.com

[14] *Microstrip Antenna Design Handbook* - R Garg, Prakash Bhartia, Inder Bahl, A Ittipiboon

[15] *The Handbook of Microstrip Antennas* - James R James

[16] *Antenna Engineering Handbook* - Richard C. Johnson.

[17]Powell's Books - *Advances in Microstrip and Printed Antennas.*

[18]. C. L. Mak, K. M. Luk, Senior Member, IEEE, K. F. Lee, Fellow, IEEE, and Y. L. Chow, "Experimental Study of a Microstrip Patch